miRNA-124 regulates palmitic acid-induced epithelial-mesenchymal transition and cell migration in human retinal pigment epithelial cells by targeting LIN7C

XIAO-DONG HAN[1*], XU-GUANG JIANG[1*], MIN YANG[1], WEN-JUN CHEN[1] and LI-GANG LI[2]

Departments of [1]Ocular Fundus Diseases and [2]Cataracts,
Xi'an Aier Ancient City Eye Hospital, Xi'an, Shaanxi 710082, P.R. China

Received October 12, 2020; Accepted March 25, 2022

DOI: 10.3892/etm.2022.11408

Abstract. The present study revealed that palmitic acid (PA) treatment induced epithelial-mesenchymal transition (EMT) of retinal pigment epithelial (RPE) cells, which are involved in the progression of proliferative vitreoretinopathy (PVR). ARPE-19 cells were treated with PA followed by miRNA screening and EMT marker detection using qRT-PCR. Then, miR-124 mimic or inhibitor was transfected into ARPE-19 cells to explore the role of miR-124 on the EMT of ARPE-19 cells using transwell assay. The underlying mechanism of miRNA were predicted by bioinformatics method and confirmed by luciferase activity reporter assay. Furthermore, gain-of-function strategy was also used to explore the role of LIN7C in the EMT of ARPE-19 cells. The expression of miRNA or mRNA expression was determined by qRT-PCR and the protein expression was determined using western blot assay. The result presented that PA reduced the expression of E-cadherin/ZO-1 whilst increasing the expression of fibronectin/α-SMA. In addition, PA treatment enhanced the expression of microRNA (miR)-124 in ARPE-19 cells. Overexpression of miR-124 enhanced PA-induced upregulation of E-cadherin and ZO-1 expression and downregulation of fibronectin and α-SMA. Moreover, miR-124 mimic also enhanced the migration of ARPE-19 cells induced by PA treatment. Inversely, miR-124 inhibitor presented opposite effect on PA-induced EMT and cell migration in ARPE-19 cells. Luciferase activity reporter assay confirmed that Lin-7 homolog C (LIN7C) was a direct target of miR-124 in ARPE-19 cells. Overexpression of LIN7C was found to suppress the migration ability and expression of fibronectin and α-SMA, while increasing expression of E-cadherin and ZO-1; miR-124 mimic abrogated the inhibitive effect of LIN7C on the EMT of ARPE-19 cells and PA further enhanced this abolishment. Collectively, these findings suggest that miR-124/LIN7C can modulate EMT and cell migration in RPE cells, which may have therapeutic implications in the management of PVR diseases.

Correspondence to: Professor Li-Gang Li, Department of Cataracts, Xi'an Aier Ancient City Eye Hospital, 59 Ziqiang West Road, Lianhu, Xi'an, Shaanxi 710082, P.R. China
E-mail: 2636964368@qq.com

Professor Xiao-Dong Han, Department of Ocular Fundus Diseases, Xi'an Aier Ancient City Eye Hospital, 59 Ziqiang West Road, Lianhu, Xi'an, Shaanxi 710082, P.R. China
E-mail: redaimexiao@163.com

*Contributed equally

Key words: proliferative vitreoretinopathy, microRNA-124, lin-7 homolog C, epithelial mesenchymal transition

Introduction

Proliferative vitreoretinopathy (PVR) is a rare ocular inflammatory disease that can result in vision loss or even blindness (1,2). Treatment strategies for PVR has drastically improved over the past decade owing to advances in surgical techniques, such as gauge vitrectomy, scleral buckling, as well as three-dimensional mediated ophthalmic surgery (3). However, PVR remains the most common cause of recurring retinal detachment, occurring in 5-10% of all cases (4). Therefore, it is of great significance to understand the mechanism underlying PVR development to devise novel therapeutic strategies.

PVR development is dependent on the proliferation and migration of retinal pigment epithelial (RPE) cells, which forms the main component of PVR membranes (5). Mounting evidence has demonstrated that RPE cells can serve fibrotic roles in promoting PVR development (6-8). Mesenchymal-like RPE cells that underwent epithelial-to mesenchymal transition (EMT) have enhanced capability of proliferation, migration and invasion (9,10). This population of RPE cells is associated with the progression of PVR (9,10). Therefore, investigating the regulation of EMT in RPE cells may provide a potential therapeutic target for PVR treatment.

Palmitic acid (PA) is a long-chain saturated fatty acid found in palm oil that has multiple reported biological and nutritional effects (11,12). Wang *et al* (13) previously reported that saturated PA can induce myocardial inflammation by binding to the toll-like receptor 4 accessory protein myeloid differentiation factor 2. In colorectal cancer, PA

can increase tumor cell proliferation in a β_2-adrenergic receptor-dependent manner (14). In addition, PA can inhibit macrophage-mediated EMT in colorectal cancer (15). A previous study also demonstrated that PA can protect RPE cells against 4-hydroxynonenal-mediated stress and light-mediated retinal degeneration in mice (16). However, the function of PA in RPE cells and the development of PVR remain poorly understood at present.

MicroRNAs (miRNAs/miRs) belong to a group of small non-coding RNAs that are involved in various biological processes, including PVR (17,18). Accumulating evidence has demonstrated that miRNAs can induce or inhibit the EMT process in RPE cells (19,21). In addition, miRNAs, such as miR-182 and miR-34a, have been reported to modulate RPE cell proliferation and migration (20,22). Consequently, augmenting understanding into the miRNA-mediated regulation and function in RPE cells can potentially facilitate the development of miRNA manipulators to reverse the progression of PVR.

According to the aforementioned literature, miRNAs and their associated mechanisms might play critical role in the regulation of RPE cell activity during PVR. The present study aimed to explore the underlying mechanism of PA mediated miR-124 dysregulation on the EMT in ARPE-19 cells. In addition, the underlying target of miR-124 was investigated to further reveal the biofunction of miR-124 in the EMT of ARPE-19 cells. According to these investigations, we hope to provide more information in the understanding and therapeutic insights in PVR diseases.

Materials and methods

Cell culture and treatment. The human RPE cell line ARPE-19 was purchased from American Type Culture Collection. The cells were cultured in DMEM supplemented with 10% FBS (both Gibco; Thermo Fisher Scientific, Inc.), 100 U/ml penicillin and 100 μg/ml streptomycin (Thermo Fisher Scientific, Inc.) in a 5% CO_2 incubator at 37˚C. PA was purchased from MilliporeSigma and dissolved in 100% ethanol. The ARPE-19 cells were treated with PA at the indicated concentrations (0, 50, 100 200, and 400 μM) at 37˚C for 48 h and cells treated with equal volume of 100% ethanol was used as the control group.

Transfection. miR-124 mimic (50 nM; 5'-CGUGUUCAC AGCGGACCUUGAU-3'), negative control mimic (NC mimic; 50 nM; 5'-AUUGGAACGAUACAGAGAAGAUU-3'), miR-124 inhibitor (50 nM; 5'-AUCAAGGUCCGCUGUGAA CACG-3') and the NC inhibitor (50 nM; 5'-UUGUACUAC ACAAAAGUACUG-3') were purchased from Invitrogen (Thermo Fisher Scientific, Inc.). For knocking down LIN7C in ARPE-19 cells, short interfering (si)RNAs targeting LIN7C (100 nM; si-LIN7C #1, 5'-GGCTACTGTTGCTGCATT TGC-3'; si-LIN7C #2, 5'-GACCTAATACATTTCAAAACT TG-3'; and si-LIN7C #3, 5'-GGGAATTTGAGAAATATTTCA TT-3' cloned into pLKO vector) and non-targeting sequence, si-NC, (100 nM; 5'-TAAGGCTATGAAGAGATAC-3') were obtained from Guangzhou RiboBio Co., Ltd. Overexpression plasmid pcDNA3.1-LINC7C (100 nM) and pcDNA3.1 (control plasmid; 100 nM) were purchased from Shanghai GenePharma Co., Ltd. Transfection was performed in ARPE-19 cells with 70% confluency using Lipofectamine® 2000 (Invitrogen; Thermo Fisher Scientific, Inc.) according to the manufacturer's guidelines at 37˚C for 48 h. Following incubation at 37˚C for 48 h, cells were harvested for the following experiments.

Reverse transcription-quantitative (RT-qPCR). RNA was extracted from the transfected/PA treated ARPE-19 cells using AccuRef Cell/Tissue Total RNA isolation kit (cat. no. AM0041; AccuRef Diagnostics; Applied StemCell, Inc.) and reverse-transcribed into complementary DNA using PrimeScript™ RT reagent kit (Takara) at 37˚C for 15 min, 85˚C for 5 sec and 4˚C for 15 min. qPCR was performed using SYBR® Green PCR Master Mix (Applied Biosystems; Thermo Fisher Scientific, Inc.) with the following conditions: 95˚C for 10 min, 40 cycles of 95˚C for 10 sec and 57˚C for 20 sec, and 72˚C for 15 sec. The relative expression levels of miRNAs and genes were calculated using the $2^{-\Delta\Delta Cq}$ method (23) and GAPDH/U6 were used as the internal controls. The primers designed by the Primer Premier 5 software (PREMIER) and used in the study are listed in Table I.

Western blotting. The cultured ARPE-19 cells were lysed using 1X CST lysis buffer (Cell Signaling Technology, Inc.) supplemented with the proteinase inhibitor cocktail (Pierce; Thermo Fisher Scientific, Inc.). Total proteins were extracted and the protein concentration was determined using a BCA protein quantification kit (Pierce; Thermo Fisher Scientific, Inc.). Equal amounts of proteins (25 μg per lane or 10 μg per lane for LIN7C overexpression assay) were separated using 12% SDS-PAGE and transferred onto polyvinylidene difluoride membranes (MilliporeSigma). The membranes were blocked with 5% non-fat milk at room temperature for 1 h and then incubated with primary antibodies overnight at 4˚C. The following primary antibodies from Abcam were used: Zonula occludens protein 1 (ZO-1; 1:1,000; cat. no. ab216880), E-cadherin (1:10,000; cat. no. ab40772), α-smooth muscle actin (SMA; 1:500; cat. no. ab124964), and fibronectin (1:1,000; cat. no. ab2413). In addition, LIN7C (1:1,000; cat. no. SAB2101347) was purchased from Sigma-Aldrich (Merck KGaA). To control sample loading, the membranes were stripped with the western blotting stripping buffer (AccuRef Diagnostics; Applied StemCell, Inc.) and re-probed with the anti-mouse GAPDH antibody from Abcam (1:10,000; cat. no. ab181602) at room temperature for 1.5 h. The membranes were washed and incubated with a HRP-conjugated goat anti-mouse (1:5,000; cat. no. ab47827; Abcam) or anti-rabbit (1:5,000; cat. no. ab7090; Abcam) secondary antibody at room temperature for 1 h and then visualized using an enhanced chemiluminescence kit (Pierce; Thermo Fisher Scientific, Inc.). With GAPDH as the internal control, the relative expression of protein bands was quantified using Image J Software (Version 1.5; National Institutes of Health).

Transwell assay. Cell migration was analyzed with a Transwell assay using a Transwell chamber (8-μm pores; Corning, Inc.). Transfected/PA-treated ARPE-19 cells were resuspended in a serum-free DMEM and added into the upper chamber at a density of $2x10^4$ per well. DMEM supplemented with 10% FBS was then added into the lower chamber. After incubation for 24 h at 37˚C, cells that migrated through the membrane were fixed by 4% paraformaldehyde at room temperature for 15 min and

Table I. Primers used in the present study.

Protein	Forward (5'-3')	Reverse (5'-3')
E-cadherin	GCTCGCTGAACTCCTCTGA	TCGCCGCCACCATACATA
ZO-1	CGGTCCTCTGAGCCTGTAAG	GGATCTACATGCGACGACAA
α-SMA	CCACTGCTGCTTCCTCTTC	CGCCGACTCCATTCCAAT
Fibronectin	GTGTCCTCCTTCCATCTTC	CAGACTGTCGGTACTCACG
LIN7C	AACGCTACTGCAAAGGCTACT	TGAATCCAAGGCCCTCTTCTG
MRPS33	TTCTCTGCTCATCACACGGC	GGCAAGGAGTTAGAGTTCCGTAT
PAGR1	GCGAAGAGGAGAGATCCGATG	GTGGGCATGTGTGGTTTTTCC
TSPAN8	AGTGCCCCAGGAGCTATGA	AGATTTCTGTATCCACGGACATTTA
NABP1	CGCGCCTGTCCCAATATGA	TTGGTCACGCGTCCTATCTC
SPIN1	CTCCCTGATAGAGTTGCGACA	AGACCATTCCCCTCCACTCA
AZI2	CTTCGAAGAAACCGGAAGCC	GCATCCATGACAACCAGAAGC
NOA1	TTTCCTCTGCAGGTTGGGTT	GGTGTATAGCCTCGGAGATGC
TXNRD1	CGCCGTAGGTCAGCTAAAGAT	GAAGCAGGGCTCTGGAGTCT
GAPDH	ACGGCAAGTTCAACGGCACAG	GAAGACGCCAGTAGACTCCACGAC
miR-124	CGUGUUCACAGCGGACCUUGAU	Universal PCR Reverse Primer (cat. no. B532451; Sangon Biotech Co., Ltd.)
miR-23b	ATCACATTGCCAGGGATTACCAC	Universal PCR Reverse Primer (cat. no. B532451; Sangon Biotech Co., Ltd.)
miR-221	AGCTACATTGTCTGCTGGGTTTC	Universal PCR Reverse Primer (cat. no. B532451; Sangon Biotech Co., Ltd.)
miR-124	TAAGGCACGCGGTGAATGCCAA	Universal PCR Reverse Primer (cat. no. B532451; Sangon Biotech Co., Ltd.)
U6	CGCTTCGGCAGCACATATACT	GAATTTGCGTGTCATCCTTGC

ZO-1, zonula occludens protein 1; α-SMA, α-smooth muscle actin; LIN7C, lin-7 homolog C; MRPS33, mitochondrial ribosomal protein 33; PAGR1, PAXIP1 associated glutamine rich protein 1; TSPAN8, tetraspanin 8; NABP1, nucleic acid binding protein 1; SPIN1, spindling 1; AZI2, 5-azacytidine induced 2; NOA1, nitric oxide associated 1; TXNRD1, thioredoxin reductase 1; miR, microRNA.

stained with 0.1% crystal violet at room temperature for 15 min (Sigma-Aldrich; Merck KGaA). The migrating cells were then imaged in a light microscope at 200x and counted manually.

Prediction of miRNA targets. The targets of miR-124 were predicted by TargetScan (https://www.targetscan.org/vert_72/), miRDB (http://mirdb.org/index.html), and microT (https://mrmicrot.imsi.athenarc.gr/?r=mrmicrot/index) online Tools. Then, the shared targeted genes were screened using the Venn analysis (https://bioinfogp.cnb.csic.es/tools/venny/) and presented in a Venn diagram.

Luciferase reporter assay. The ARPE-19 cells were seeded into 24-well plates at a density of $5.0x10^5$ per well. Subsequently, 24 h later, luciferase reporter vector psiCHECK2 (Promega Corporation) containing the wild-type or mutant (0.25 μg each) 3'-untranslated regions (UTR) of LIN7C, purchased from Guangzhou RiboBio Co., Ltd, was transiently co-transfected with miR-124 mimics (100 nM) or NC (100 nM) into ARPE-19 cells using Lipofectamine 2000 (Invitrogen; Thermo Fisher Scientific, Inc.) according to the manufacturer's protocol at 37˚C for 24 h. At 24 h post-transfection, the relative luciferase activity was analyzed using a Dual-Luciferase Reporter Assay System with *Renilla* luciferase activity as the internal control (Promega Corporation).

Prediction of miR-124 using bioinformatics. The underlying targets of miR-124 were predicted using TargetScan (targetscan.org/vert_72/), miRDB (http://mirdb.org/index.html), and microT (https://dianalab.e-ce.uth.gr/html/dianauniverse/index.php?r=microT_CDS) online databases with their default parameters. Then, the shared targets among these three databases were screened using Venn analysis.

Statistical analysis. All experiments were performed in triplicate and the results are presented as the mean ± standard deviation. Statistical analysis was performed using GraphPad prism (version 8.0; GraphPad Software, Inc.). Unpaired student's t-test or one-way analysis of variance followed by Tukey's post hoc test was performed to analyze the differences among ≥ two groups. $P<0.05$ was considered to indicate a statistically significant difference.

Results

PA treatment induces EMT and enhances miR-124 expression in ARPE-19 cells. To investigate the function of PA in EMT and the underlying mechanism, ARPE-19 cells were treated with PA at different concentrations (0, 50, 100, 200 and 400 μM) for 48 h. The results revealed that PA treatment decreased the protein expression levels of E-cadherin and ZO-1

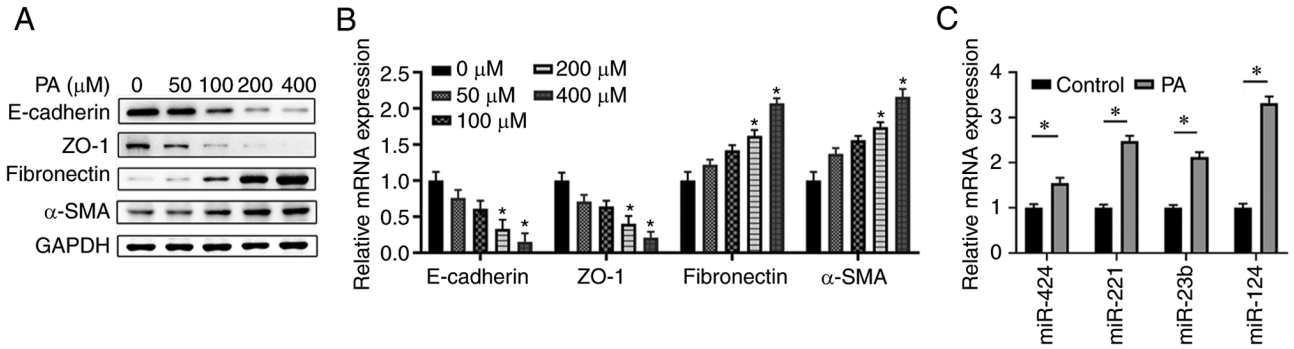

Figure 1. PA treatment induces EMT and increases miR-124 expression in ARPE-19 cells. ARPE-19 cells were treated with PA at different concentrations (0, 50, 100, 200 and 400 μM) for 48 h. (A) Protein and (B) mRNA expression levels of the key molecules in EMT (E-cadherin, ZO-1, fibronectin and α-SMA) were measured using western blotting and RT-qPCR. (C) ARPE-19 cells were treated with 200 μM PA for 48 h, before the expression of miR-424, miR-221, miR-23b and miR-124 were analyzed using RT-qPCR. *P<0.05 vs. 0 μM/control group. PA, palmitic acid; EMT, epithelial mesenchymal transition; miR, microRNA; RT-qPCR, reverse transcription-quantitative PCR; ZO-1, zonula occludens protein 1; α-SMA, α-smooth muscle actin.

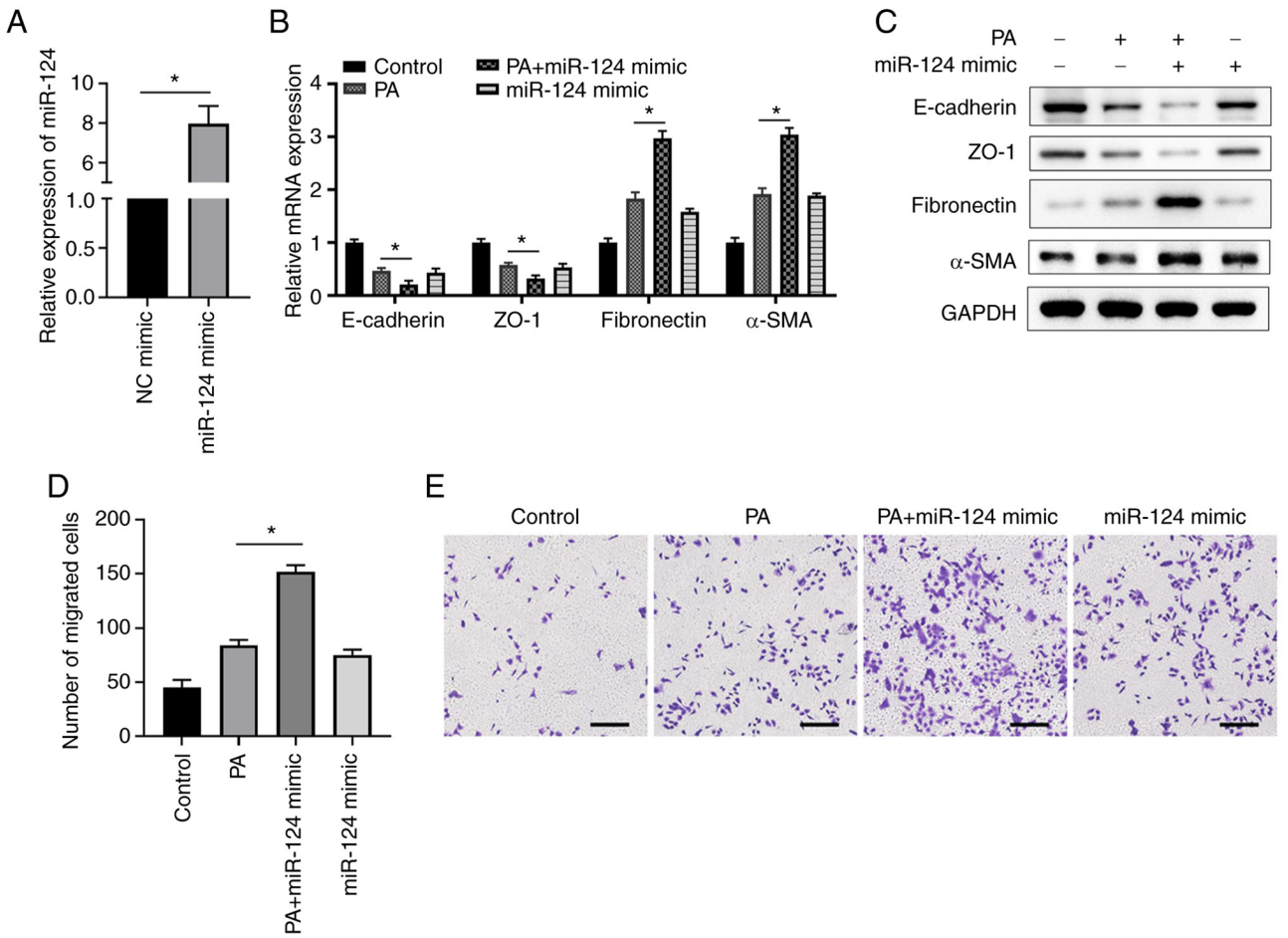

Figure 2. miR-124 overexpression enhances PA-induced EMT and cell migration in ARPE-19 cells. (A) ARPE-19 cells were transfected with either the miR-124 mimics or NC, before the expression levels of miR-124 were determined at 48 h after transfection by RT-qPCR. (B) mRNA and (C) protein expression levels of the key molecules in EMT (E-cadherin, ZO-1, fibronectin and α-SMA) were measured using RT-qPCR and western blotting, respectively. (D and E) ARPE-19 cells were transfected with miR-124 mimics or NC and/or cultured in the presence or absence of 200 μM PA. Cells migration was analyzed using Transwell assay. (D) Number of migrated cells in the different groups was calculated and (E) representative images of Transwell cell migration assays are presented; scale bar=200 μm. *P<0.05. PA, palmitic acid; EMT, epithelial mesenchymal transition; miR, microRNA; RT-qPCR, reverse transcription-quantitative PCR; ZO-1, zonula occludens protein 1; α-SMA, α-smooth muscle actin; NC, negative control.

whilst increasing the protein expression levels of fibronectin and α-SMA in a dose-dependent manner (Fig. 1A). Similarly, treatment with 200 μM PA significantly suppressed the mRNA expression levels of E-cadherin and ZO-1 but increased those of fibronectin and α-SMA in ARPE-19 cells compared with the control (Fig. 1B). RT-qPCR found that although miR-424, miR-221 and miR-23b expression was significantly enhanced upon PA treatment, the increase in miR-124 expression was

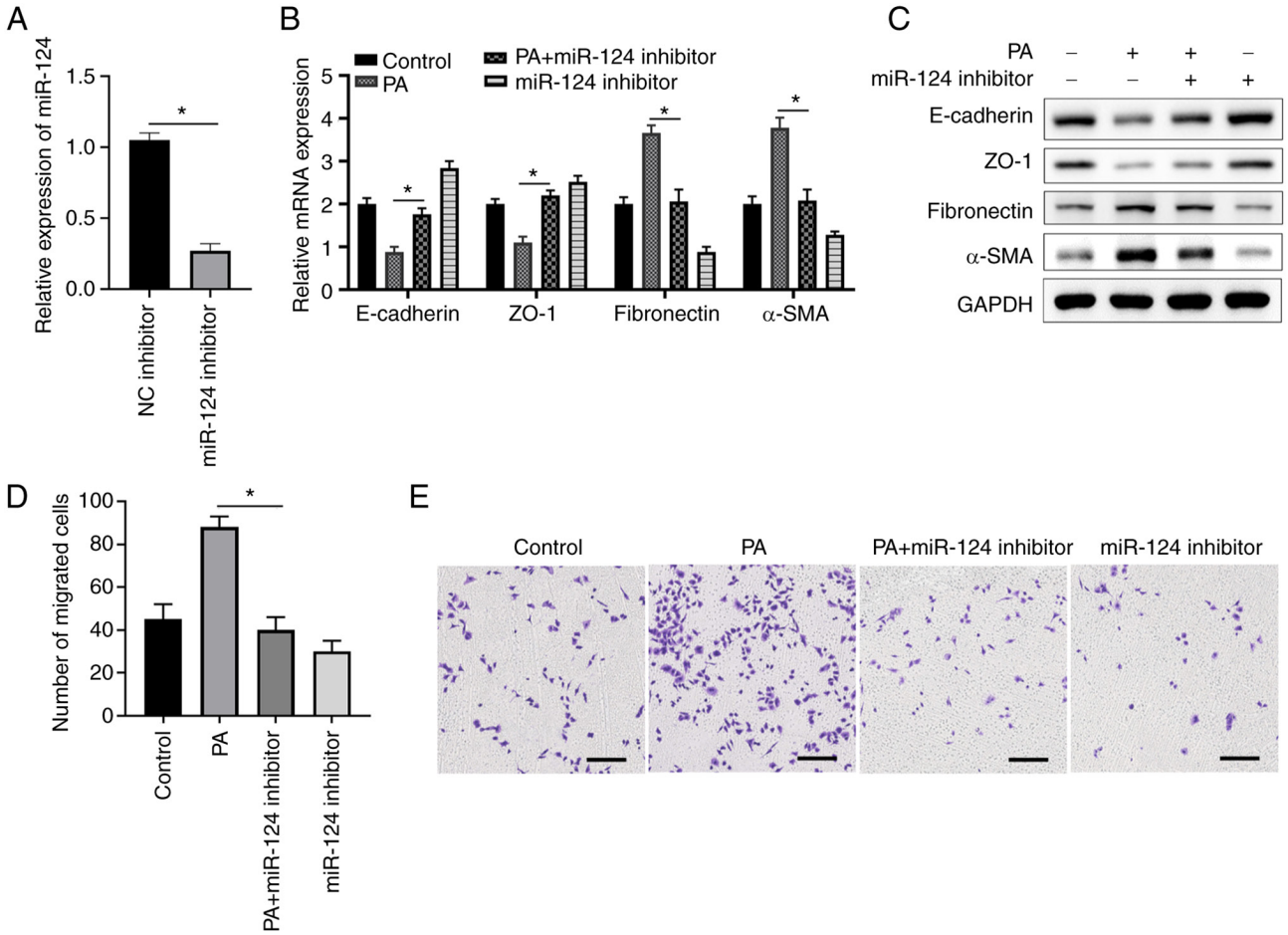

Figure 3. miR-124 knockdown suppresses PA-induced EMT and cell migration in ARPE-19 cells. (A) ARPE-19 cells were transfected with either the miR-124 inhibitor or NC, before the expression levels of miR-124 were determined at 48 h post-transfection using RT-qPCR. (B) mRNA and (C) protein levels of the key molecules in EMT (E-cadherin, ZO-1, fibronectin and α-SMA) were determined using RT-qPCR and western blotting, respectively. (D and E) ARPE-19 cells were transfected with miR-124 inhibitor or NC and/or cultured in the presence or absence of 200 μM PA before cell migration was analyzed using a Transwell assay. (D) Number of migrated cells in different groups were calculated and (E) representative images of Transwell cell migration assays are presented; scale bar=200 μm. *P<0.05. PA, palmitic acid; EMT, epithelial mesenchymal transition; miR, microRNA; RT-qPCR, reverse transcription-quantitative PCR; ZO-1, zonula occludens protein 1; α-SMA, α-smooth muscle actin; NC, negative control.

the highest expression compared with that in the control group (Fig. 1C). Taken together, these data suggested that miR-124 may be involve in PA-induced EMT of ARPE-19 cells; therefore, the present study focused on the role of miR-124 in EMT and its regulation by PA treatment.

Overexpression of miR-124 enhances PA-induced EMT and cell migration in ARPE-19 cells. Next, the possible function of miR-124 in EMT was explored, where ARPE-19 cells were transfected with either the NC or miR-124 mimics. Overexpression of miR-124, which was confirmed by RT-qPCR compared with that in corresponding control cells transfected with the NC mimic (Fig. 2A), mediated a similar effect to PA treatment. Specifically, miR-124 mimic transfection markedly decreased the expression of E-cadherin and ZO-1 but enhanced the expression of fibronectin and α-SMA on both mRNA and protein levels compared with those in the control group (Fig. 2B and C). Subsequently, overexpression of miR-124 together with PA treatment resulted in the lowest expression levels of E-cadherin and ZO-1 but the highest expression levels of fibronectin and α-SMA in ARPE-19 cells (Fig. 2B and C). All of these observations were significant compared with those in the PA-only group (Fig. 2B and C). In addition, it was observed that miR-124 mimics transfection or PA treatment markedly enhanced ARPE-19 cell migration compared with that in the control (Fig. 2D and E). By contrast, the overexpression of miR-124 significantly enhanced the cell migration of ARPE-19 cells treated with PA compared with that in cells treated with PA only (Fig. 2D and E). These findings suggest that miR-124 accelerated migration ability of ARPE-19 cells to promote PA-induced EMT.

Knocking down miR-124 expression suppresses PA-induced EMT and cell migration in ARPE-19 cells. Furthermore, a loss-of-function assay was performed using a miR-124 inhibitor to investigate the function of miR-124. Transfection with the miR-124 inhibitor significantly suppressed the expression of miR-124 compared with that in cells transfected with the NC inhibitor (Fig. 3A). PA treatment decreased the expression of E-cadherin and ZO-1 whilst enhancing the expression of fibronectin and α-SMA compared with those in the control group, transfection with the miR-124 inhibitor resulted in the opposite effects (Fig. 3B and C). In the PA + miR-124

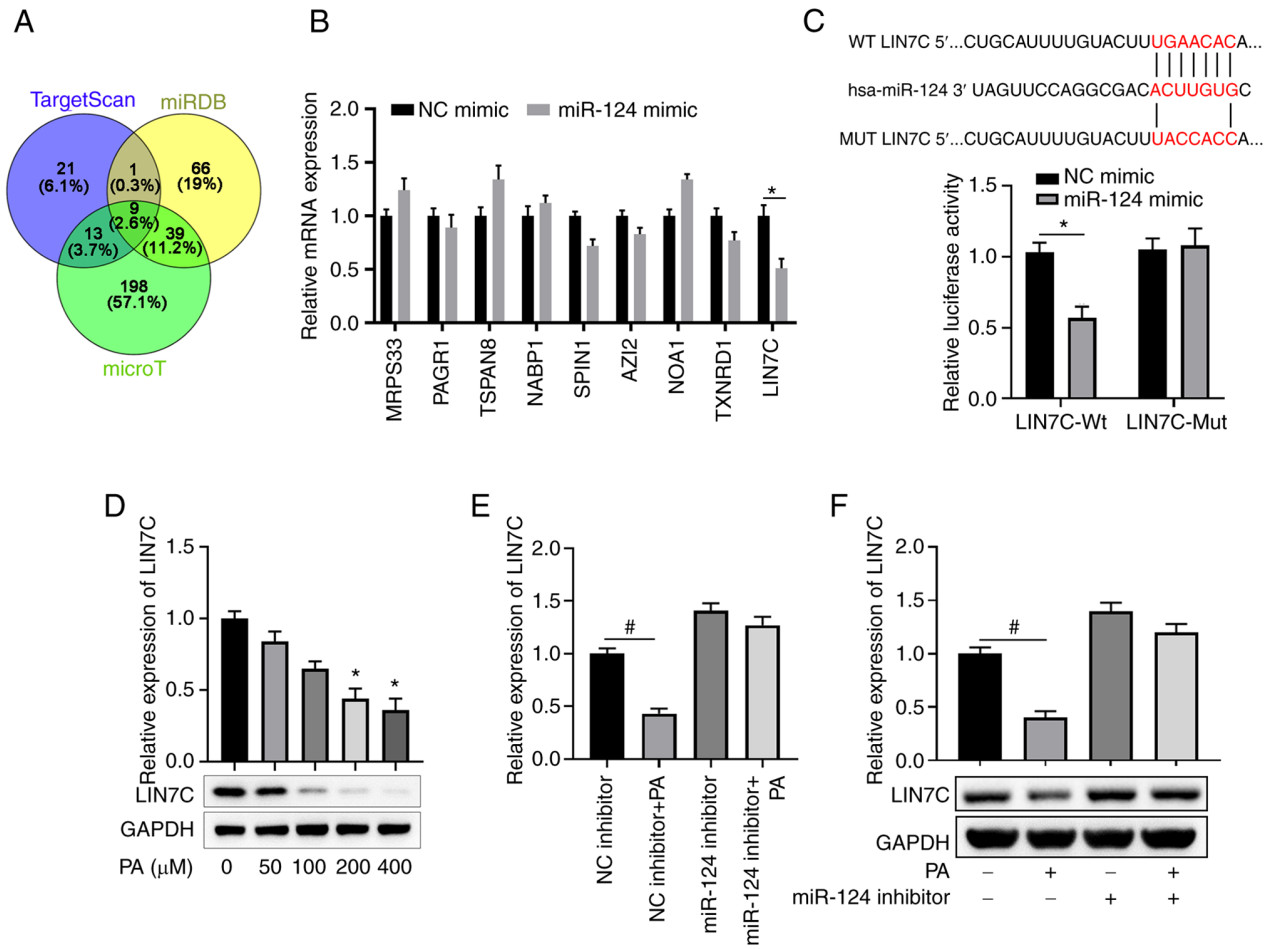

Figure 4. LIN7C is a direct target of miR-124 in ARPE-19 cells. (A) Venn diagram presents the numbers of candidate mRNA targets of miR-124 predicted using three public algorithms TargetScan, miRDB and micro-T. (B) ARPE-19 cells were transfected with NC or miR-124 mimics. The mRNA expression levels of the indicated candidate targets of miR-124 were analyzed using RT-qPCR 48 h later. (C) Diagrams show the putative binding sites between miR-124 and corresponding WT or MUT sites of LIN7C 3'UTR. ARPE-19 cells were co-transfected with reporter vector containing WT or MUT LIN7C 3'-UTR, together with NC or miR-124 mimics. Dual luciferase activity was detected in ARPE-19 cells at 48 h post transfection. (D) Protein expression levels of LIN7C in ARPE-19 cells treated with PA at the indicated concentrations were determined by western blotting. (E and F) ARPE-19 cells were transfected with NC or miR-124 inhibitor with or without 200 μM PA treatment. At 48 h later, (E) mRNA and (F) expression protein levels of LIN7C in each treatment group were measured using RT-qPCR and western blot assays, respectively. *P<0.05 vs. NC mimic; $^{\#}$P<0.05 vs. NC inhibitor. LIN7C, lin-7 homolog C; miR, microRNA; NC, negative control; RT-qPCR, reverse transcription-quantitative PCR; WT, wild-type; MUT, mutant; UTR, untranslated region; PA, palmitic acid.

inhibitor group, miR-124 inhibitor transfection was also found to antagonize the effect of PA treatment, resulting in the E-cadherin, ZO-1, fibronectin and α-SMA expression levels in ARPE-19 cells returning to those comparable with the control group (Fig. 3B and C). In addition, transfection with the miR-124 inhibitor was revealed to markedly inhibit ARPE-19 cell migration compared with the control, whereas miR-124 inhibition significantly reversed the PA-enhanced ARPE-19 cell migration (Fig. 3D and E). These findings indicate that PA enhances the EMT of ARPE-19 cells via miR-124 and inhibition of miR-124 abrogated EMT of ARPE-19 cells induced by PA.

LIN7C is a direct target of miR-124 in ARPE-19 cells. To explore the mechanism by which miR-124 regulates EMT in ARPE-19 cells, bioinformatics analyses were performed to predict the potential targets of miR-124 using TargetScan, miRDB, and micro-T (Fig. 4A). A total of nine potential targets were predicted by all three tools (Fig. 4A). ARPE-19 cells were then transfected with miR-124 mimics or NC, before the relative expression of these potential target genes were analyzed 48 h later. As presented in Fig. 4B, transfection of miR-124 mimics significantly suppressed the expression of LIN7C compared with that in the NC group. There were also complementary binding sequences between miR-124 and the 3'-UTR of LIN7C (Fig. 4C). Luciferase reporter assay subsequently confirmed that miR-124 mimic could significantly decrease the luciferase activity of LIN7C-Wt but had no effect on the activity of LIN7C-Mut, suggesting a direct interaction between miR-124 and LIN7C (Fig. 4C). PA treatment was also confirmed to suppress LIN7C expression in a dose-dependent manner, with this reduction reaching significance at 200 and 400 μM compared with that in the 0 μM group (Fig. 4D). Furthermore, inhibition of miR-124 expression markedly enhanced the expression of LIN7C in ARPE-19 cells compared with the NC inhibitor group, whilst miR-124 inhibitor transfection reversed the suppressive effects of PA treatment on LIN7C expression (Fig. 4E and F). All of these findings indicate that LIN7C is a target of miR-124 in ARPE-19 cells.

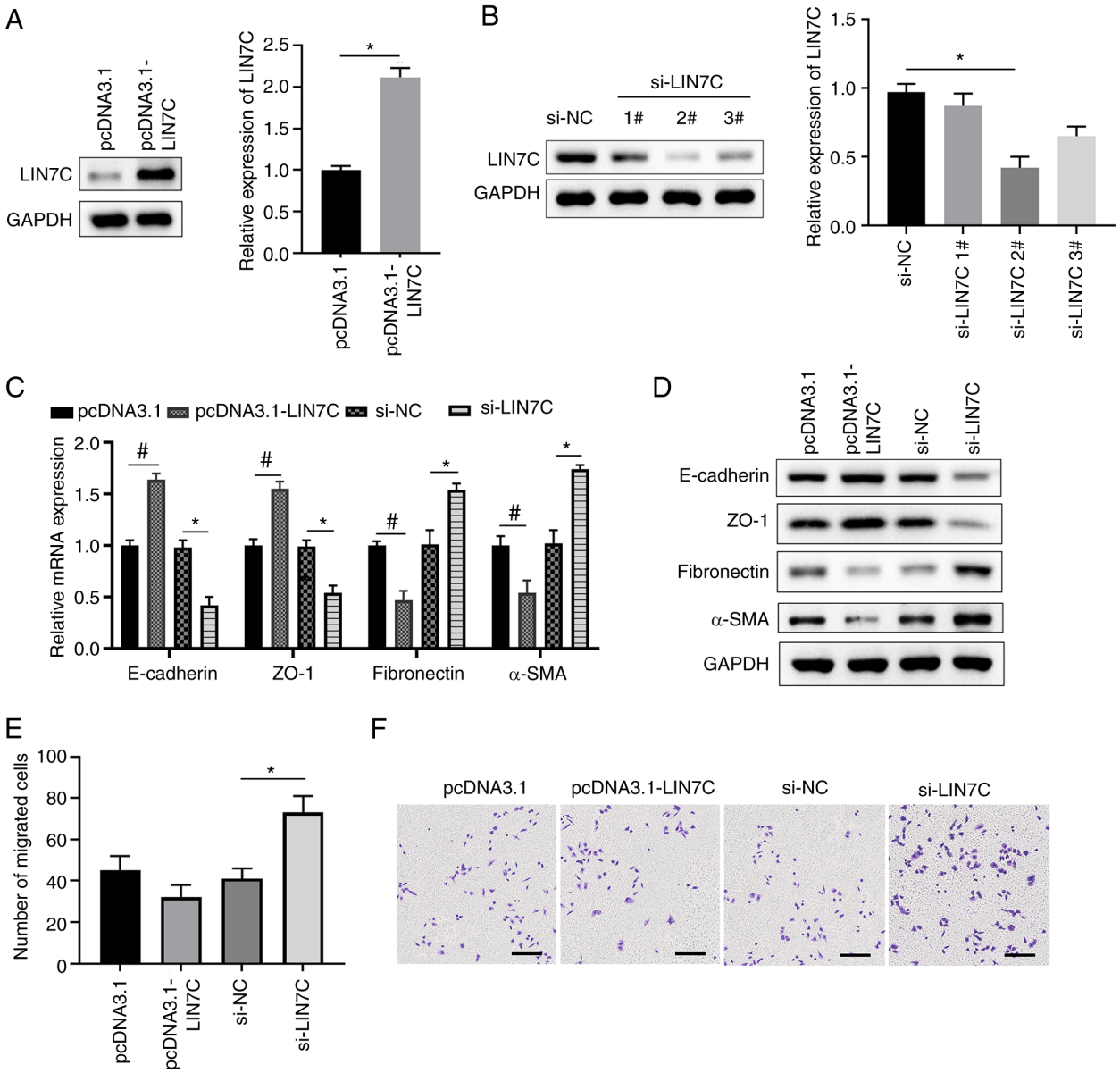

Figure 5. LIN7C regulates EMT and cell migration in ARPE-19 cells. (A) ARPE-19 cells were transfected with control empty plasmids or LIN7C-overexpressing plasmids. Protein and mRNA expression levels of LIN7C in ARPE-19 cells were determined using western blotting and RT-qPCR, respectively. (B) ARPE-19 cells were transfected with si-NC or LIN7C-specific siRNA oligos. Protein and mRNA expression levels of LIN7C in ARPE-19 cells were then determined using western blotting and RT-qPCR assays, respectively. (C-F) ARPE-19 cells were transfected with control empty plasmids or LIN7C-overexpressing plasmids, si-NC or si-LIN7C #2. Expression levels of the key molecules in EMT (E-cadherin, ZO-1, fibronectin and α-SMA) were determined using (C) RT-qPCR for mRNA and (D) western blotting for proteins. At 48 h post-transfection, ARPE-19 cells were cultured in Transwell chambers and migratory cells were stained with crystal-violet. (E) The number of migrated cells in one field of view in each group is quantified and (F) representative images of the Transwell cell migration assays are presented; scale bar, 200 μm. *P<0.05 and $^{\#}$P<0.05. EMT, epithelial mesenchymal transition; RT-qPCR, reverse transcription-quantitative PCR; ZO-1, zonula occludens protein 1; α-SMA, α-smooth muscle actin; NC, negative control; LIN7C, lin-7 homolog C; NC, negative control; si, short-interfering.

LIN7C regulates EMT and cell migration in ARPE-19 cells. To study the effect of LIN7C on EMT, the overexpression vector for LIN7C was constructed and transfected into ARPE-19 cells to overexpress LIN7C, which was successful compared with that in cells transfected with the empty pcDNA3.1 vector (Fig. 5A). By contrast, siRNAs targeting LIN7C were transfected into ARPE-19 cells to silence the expression of LIN7C. The result suggested that si-LIN7C 2# and 3# significantly decrease LIN7C expression, and si-LIN7C 3# presented a more effective effect than si-LIN7C 2# (Fig. 5B). Therefore, si-LIN7C 2# was selected and used for the following experiments. The overexpression of LIN7C was demonstrated to suppress EMT, with markedly enhanced expression levels of E-cadherin/ZO-1 and markedly decreased expression levels of fibronectin/α-SMA compared with those in the empty vector control group (Fig. 5C and D). Knockdown of LIN7C significantly enhanced EMT, namely significantly inhibiting expression of E-cadherin and ZO-1 but enhancing expression of fibronectin and α-SMA compared with the si-NC group (Fig. 5C and D). Furthermore, overexpression of LIN7C was demonstrated to markedly inhibit cell migration compared with that in the empty vector group, whilst its knockdown significantly enhanced cell migration compared with that in the si-NC group (Fig. 5E and F). Taken together, these

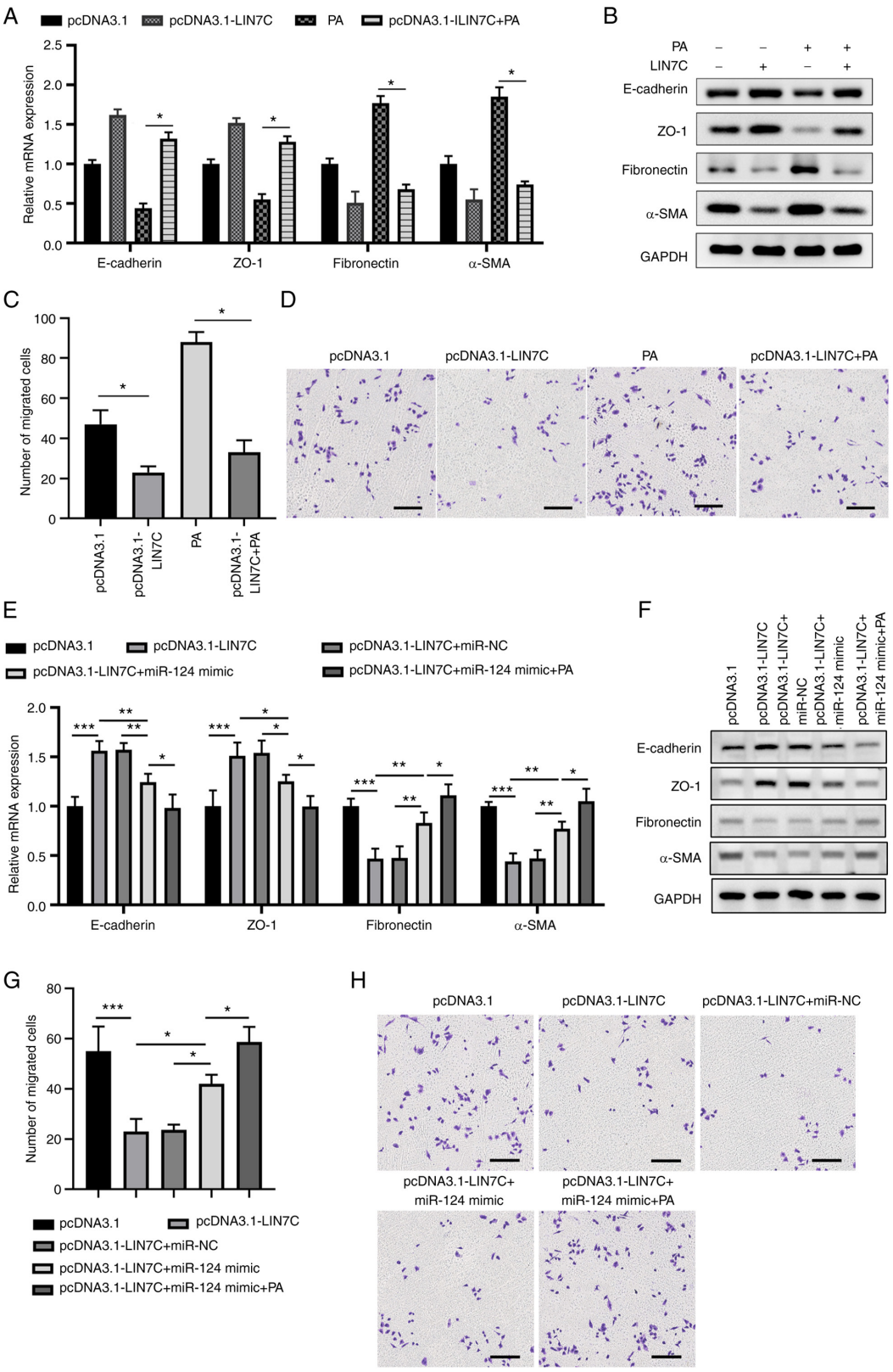

Figure 6. Overexpression of LIN7C abrogates PA-induced EMT and cell migration in ARPE-19 cells. ARPE-19 cells were transfected with control vector, pLIN7C and/or treated with or without 200 μM PA. EMT-associated markers and migration in the cells were determined 48 h later. Expression levels of key molecules in EMT (E-cadherin, ZO-1, fibronectin and α-SMA) were determined using (A) RT-qPCR for mRNA and (B) western blotting for proteins. (C and D) ARPE-19 cells were transfected with control or pLIN7C and/or cultured in the presence or absence of 200 μM PA. Cell migration was analyzed using a Transwell assay. (C) Number of migrated cells in different groups were calculated and (D) representative images from Transwell cell migration assays are presented; scale bar, 200 μm. (E-H) ARPE-19 cells were transfected with pcDNA3.1 or pcDNA3.1-LIN7 and miR-NC or miR-124 followed by 200 μM PA treatment, before EMT-associated marker expression and cell migration were measured 48 h later. Expression levels of the key molecules in EMT (E-cadherin, ZO-1, fibronectin and α-SMA) were determined using (E) RT-qPCR for mRNA and (F) western blotting for proteins. (G) Number of migrated cells in the different groups were calculated and (H) representative images of Transwell cell migration assays are presented; scale bar, 200 μm. *P<0.05, **P<0.01, ***P<0.001. PA, palmitic acid; EMT, epithelial mesenchymal transition; miR, microRNA; RT-qPCR, reverse transcription-quantitative PCR; ZO-1, zonula occludens protein 1; α-SMA, α-smooth muscle actin; NC, negative control; LIN7C, lin-7 homolog C.

results indicate that silencing LIN7C significantly promoted migration of ARPE-19 cells.

Overexpression of LIN7C abrogates PA-induced EMT and cell migration in ARPE-19 cells. To further investigate the role of LIN7C in EMT, the APRE-19 cells were transfected either with the control vector or the overexpression vector for LIN7C, with or without PA treatment. PA treatment was found to induce EMT compared with the pcDNA3.1 group, as demonstrated by decreased expression levels of E-cadherin and ZO-1 and enhanced expression levels of fibronectin and α-SMA (Fig. 6A and B). By contrast, overexpression of LIN7C markedly reversed the PA-induced EMT in ARPE-19 cells compared with that in the PA-only group (Fig. 6A and B). Overexpression of LIN7C also significantly suppressed cell migration compared with that in the empty vector group, whereas PA treatment produced the opposite effect. However, LIN7C overexpression significantly reduced PA-induced cell migration in ARPE-19 cells compared with the PA group (Fig. 6C and D). In addition, overexpression of miR-124 markedly reversed the upregulation of E-cadherin and ZO-1 and the downregulation of fibronectin and α-SMA previously mediated by LIN7C overexpression, which were in turn enhanced by PA treatment (Fig. 6E and F). In addition, overexpression of miR-124 significantly attenuated the inhibitory effects of LIN7C overexpression on the migration of ARPE-19 cells, which were significantly potentiated by PA treatment (Fig. 6G and H). Collectively, these data suggest that LIN7C could antagonize the EMT promotion function of PA in ARPE-19 cells.

Discussion

Accumulating evidence has demonstrated that cell proliferation, migration and EMT of RPE cells are important for PVR development (24,25). Furthermore, blocking EMT in RPE cells as been previously shown to prevent PVR pathogenesis (26). The present study revealed that PA treatment induced EMT and enhanced miR-124 expression in ARPE-19 cells. miR-124 overexpression synergistically enhanced the PA-induced EMT and cell migration in ARPE-19 cells. Furthermore, LIN7C was established as a direct target of miR-124, whereby the overexpression of LIN7C abrogated the PA-induced EMT in ARPE-19 cells. Therefore, the PA/miR-124/LIN7C functional cascade was suggested to mediate EMT and cell migration in RPE cells.

PA has been reported to regulate miRNA expression, such as miR-221 and miR-130a (27,28). Therefore, the present study performed a PA-associated miRNA microarray to analyze the differentially expressed miRNAs in ARPE-19 cells with or without PA treatment. The present study demonstrated that the expression of multiple miRNAs have been demonstrated to be regulated by PA treatment, where miR-124 was among the most upregulated miRNAs in ARPE-19 cells. Chu-Tan *et al* (29) previously revealed that the dysregulated expression of miR-124 is associated with retinal inflammation and photoreceptor death, such that miR-124 overexpression can alleviate retinal degeneration via regulating *CCL2*. The regulatory effects of miR-124 on EMT has been investigated by previous studies on triple-negative breast cancer, nasopharyngeal carcinoma, non-small cell lung cancer and clear cell renal carcinoma (30-33). Consistently, the present study revealed that the miR-124 mimics enhanced EMT in ARPE-19 cells whilst the miR-124 inhibitor suppressed PA-induced EMT. In addition, miR-124 enhanced PA-induced ARPE-19 cell migration, which may further aggravate PVR progression.

miR-124 has been studied as a potential tumor suppressor in various tumors (30,31,34). In triple-negative breast cancer and clear cell renal carcinoma, miR-124 was found to negatively regulate the expression of zinc finger E-box-binding homeobox 2 (30,31,32). Calpain small subunit 4 has been identified to be a target of miR-124, whilst long non-coding RNA metastasis-associated lung adenocarcinoma transcript 1 was documented to sponge miR-124 expression in nasopharyngeal carcinoma cells (31). The present study revealed that miR-124 regulated LIN7C expression by directly binding to the 3'-UTR of LIN7C. LIN7C has been reported to be as a dynamic marker for polarity maturation in the zebra fish retinal epithelium (35). However, to the best of our knowledge, the function of LIN7C in PVR development has not been studied previously. The present study hypothesized that LIN7C regulated EMT and cell migration in ARPE-19 cells. Overexpression of LIN7C antagonized the effect of PA treatment on EMT induction. Therefore, the miR-124/LIN7C axis, in conjunction with PA treatment, may serve a key role in the EMT and pathogenesis of PVR. Nevertheless, how LIN7C modulated the EMT process and the underlying mechanism of miR-124/LIN7C in PVR warrant further investigation.

In summary, the present study demonstrated that PA treatment induced EMT and promoted the migration of RPE cells by upregulating miR-124 expression whilst inhibiting LIN7C expression. These findings suggest that targeting miR-124/LIN7C may prove to be useful in preventing and treating PVR.

Acknowledgements

Not applicable.

Funding

No funding was received.

Availability of data and materials

The datasets used and/or analyzed during the current study available from the corresponding author on reasonable request.

Authors' contributions

XDH and LGL conceived and designed the experiments. XGJ and MY performed the experiments. WJC analyzed and interpreted the data. XDH and LGL confirm the authenticity of all the raw data. All authors read and approved the final manuscript.

Ethics approval and consent to participate

Not applicable.

Patient consent for publication

Not applicable.

Competing interests

The authors declare that they have no competing interests.

References

1. Pastor JC: Proliferative vitreoretinopathy: An overview. Surv Ophthalmol 43: 3-18, 1998.
2. Di Lauro S, Kadhim MR, Charteris DG and Pastor JC: Classifications for proliferative vitreoretinopathy (PVR): An analysis of their use in publications over the last 15 years. J Ophthalmol 2016: 7807596, 2016.
3. Coffee RE, Jiang L and Rahman SA: Proliferative vitreoretinopathy: Advances in surgical management. Int Ophthalmol Clin 54: 91-109, 2014.
4. Idrees S, Sridhar J and Kuriya AE: Proliferative vitreoretinopathy: A review. Int Ophthalmol Clin 59: 221-240, 2019.
5. Charteris DG: Proliferative vitreoretinopathy: Pathobiology, surgical management, and adjunctive treatment. Br J Ophthalmol 79: 953-960, 1995.
6. Lee SC, Kwon OW, Seong GJ, Kim SH, Ahn JE and Kay ED: Epitheliomesenchymal transdifferentiation of cultured RPE cells. Ophthalmic Res 33: 80-86, 2001.
7. Mudhar HS: A brief review of the histopathology of proliferative vitreoretinopathy (PVR). Eye (Lond) 34: 246-250, 2020.
8. Zou H, Shan C, Ma L, Liu J, Yang N and Zhao J: Polarity and epithelial-mesenchymal transition of retinal pigment epithelial cells in proliferative vitreoretinopathy. Peer J 8: e10136, 2020.
9. He H, Kuriyan AE, Su CW, Mahabole M, Zhang Y, Zhu YT, Flynn HW, Parel JM and Tseng SC: Inhibition of proliferation and epithelial mesenchymal transition in retinal pigment epithelial cells by heavy chain-hyaluronan/pentraxin 3. Sci Rep 7: 43736, 2017.
10. Tamiya S, Liu L and Kaplan HJ: Epithelial-mesenchymal transition and proliferation of retinal pigment epithelial cells initiated upon loss of cell-cell contact. Invest Ophthalmol Vis Sci 51: 2755-2763, 2010.
11. Carta G, Murru E, Banni S and Manca C: Palmitic acid: Physiological role, metabolism and nutritional implications. Front Physiol 8: 902, 2017.
12. Mancini A, Imperlini E, Nigro E, Montagnese C, Daniele A, Orrù S and Buono P: Biological and nutritional properties of palm oil and palmitic acid: Effects on health. Molecules 20: 17339-17361, 2015.
13. Wang Y, Qian Y, Fang Q, Zhong P, Li W, Wang L, Fu W, Zhang Y, Xu Z, Li X and Liang G: Saturated palmitic acid induces myocardial inflammatory injuries through direct binding to TLR4 accessory protein MD2. Nat Commun 8: 13997, 2017.
14. Fatima S, Hu X, Huang C, Zhang W, Cai J, Huang M, Gong RH, Chen M, Ho AHM, Su T, *et al*: High-fat diet feeding and palmitic acid increase CRC growth in β2AR-dependent manner. Cell Death Dis 10: 711, 2019.
15. de Araujo Junior RF, Eich C, Jorquera C, Schomann T, Baldazzi F, Chan AB and Cruz LJ: Ceramide and palmitic acid inhibit macrophage-mediated epithelial-mesenchymal transition in colorectal cancer. Mol Cell Biochem 468: 153-168, 2020.
16. Gutierrez MA, Davis SS, Rosko A, Nguyen SM, Mitchell KP, Mateen S, Neves J, Garcia TY, Mooney S, Perdew GH, *et al*: A novel AhR ligand, 2AI, protects the retina from environmental stress. Sci Rep 6: 29025, 2016.
17. Osada H and Takahashi T: MicroRNAs in biological processes and carcinogenesis. Carcinogenesis 28: 2-12, 2007.
18. Kaneko H and Terasaki H: Biological involvement of microRNAs in proliferative vitreoretinopathy. Transl Vis Sci Technol 6: 5, 2017.
19. Usui-Ouchi A, Ouchi Y, Kiyokawa M, Sakuma T, Ito R and Ebihara N: Upregulation of Mir-21 levels in the vitreous humor is associated with development of proliferative vitreoretinal disease. PLoS One 11: e0158043, 2016.
20. Wang L, Dong F, Reinach PS, He D, Zhao X, Chen X, Hu DN and Yan D: MicroRNA-182 suppresses HGF/SF-induced increases in retinal pigment epithelial cell proliferation and migration through targeting c-Met. PLoS One 11: e0167684, 2016.
21. Takayama K, Kaneko H, Hwang SJ, Ye F, Higuchi A, Tsunekawa T, Matsuura T, Iwase T, Asami T, Ito Y, *et al*: Increased ocular levels of microRNA-148a in cases of retinal detachment promote epithelial-mesenchymal transition. Invest Ophthalmol Vis Sci 57: 2699-2705, 2016.
22. Hou Q, Zhou L, Tang J, Ma N, Xu A, Tang J, Zheng D, Chen X, Chen F, Dong XD and Tu L: LGR4 is a direct target of microRNA-34a and modulates the proliferation and migration of retinal pigment epithelial ARPE-19 cells. PLoS One 11: e0168320, 2016.
23. Livak KJ and Schmittgen TD: Analysis of relative gene expression data using real-time quantitative PCR and the 2(-Delta Delta C(T)) method. Methods 25: 402-408, 2001.
24. Li X, Zhao M and He S: RPE epithelial-mesenchymal transition plays a critical role in the pathogenesis of proliferative vitreoretinopathy. Ann Transl Med 8: 263, 2020.
25. Tamiya S and Kaplan HJ: Role of epithelial-mesenchymal transition in proliferative vitreoretinopathy. Exp Eye Res 142: 26-31, 2016.
26. Nagasaka Y, Kaneko H, Ye F, Kachi S, Asami T, Kato S, Takayama K, Hwang SJ, Kataoka K, Shimizu H, *et al*: Role of Caveolin-1 for blocking the epithelial-mesenchymal transition in proliferative vitreoretinopathy. Invest Ophthalmol Vis Sci 58: 221-229, 2017.
27. Huang F, Chen J, Wang J, Zhu P and Lin W: Palmitic acid induces microRNA-221 expression to decrease glucose uptake in HepG2 cells via the PI3K/AKT/GLUT4 pathway. Biomed Res Int 2019: 8171989, 2019.
28. Gu X, Wang XQ, Lin MJ, Liang H, Fan SY, Wang L, Yan X, Liu W and Shen FX: Molecular interplay between microRNA-130a and PTEN in palmitic acid-mediated impaired function of endothelial progenitor cells: Effects of metformin. Int J Mol Med 43: 2187-2198, 2019.
29. Chu-Tan JA, Rutar M, Saxena K, Aggio-Bruce R, Essex RW, Valter K, Jiao H, Fernando N, Wooff Y, Madigan MC, *et al*: MicroRNA-124 dysregulation is associated with retinal inflammation and photoreceptor death in the degenerating retina. Invest Ophthalmol Vis Sci 59: 4094-4105, 2018.
30. Ji H, Sang M, Liu F, Ai N and Geng C: miR-124 regulates EMT based on ZEB2 target to inhibit invasion and metastasis in triple-negative breast cancer. Pathol Res Pract 215: 697-704, 2019.
31. Shi B, Wang Y and Yin F: MALAT1/miR-124/Capn4 axis regulates proliferation, invasion and EMT in nasopharyngeal carcinoma cells. Cancer Biol Ther 18: 792-800, 2017.
32. Chen J, Zhong Y and Li L: miR-124 and miR-203 synergistically inactivate EMT pathway via coregulation of ZEB2 in clear cell renal cell carcinoma (ccRCC). J Transl Med 18: 69, 2020.
33. Wu J, Weng Y, He F, Liang D and Cai L: LncRNA MALAT-1 competitively regulates miR-124 to promote EMT and development of non-small-cell lung cancer. Anticancer Drugs 29: 628-636, 2018.
34. Li Y, Yan J, Wang Y, Wang C, Zhang C and Li G: LINC00240 promotes gastric cancer cell proliferation, migration and EMT via the miR-124-3p / DNMT3B axis. Cell Biochem Funct 38: 1079-1088, 2020.
35. Luz M and Knust E: Fluorescently tagged Lin7c is a dynamic marker for polarity maturation in the zebrafish retinal epithelium. Biol Open 2: 867-871, 2013.